

Automated Wildfire Damage Assessment from Multi-view Ground-level Imagery Via Vision Language Models

Miguel Esparza¹, Archit Gupta¹, Ali Mostafavi¹, Kai Yin¹, Yiming Xiao¹*

¹ *Urban Resilience.AI Lab, Zachry Department of Civil and Environmental Engineering, Texas A&M University, College Station, TX 77840, United States of America*

**Corresponding Author: mte1224@tamu.edu*

Abstract

The escalating intensity and frequency of wildfires demand innovative computational methods for rapid and accurate property damage assessment. Traditional methods are often time-consuming, while modern computer vision approaches typically require extensive labeled datasets, hindering immediate post-disaster deployment. This research introduces a novel, zero-shot framework leveraging pre-trained vision language models (VLMs) to classify damage from ground-level imagery. We propose and evaluate two pipelines applied to the 2025 Eaton and Palisades fires in California—a VLM (Pipeline A) and a VLM + large language model (LLM) approach (Pipeline B)—that integrate structured prompts based on specific wildfire damage indicators. A primary scientific contribution of this study is demonstrating the VLMs efficacy in synthesizing information from multiple perspectives to identify nuanced damage—a critical limitation in existing literature. Our findings reveal that while single-view assessments struggled to classify *affected* structures (F1 scores ranging from 0.225 to 0.511), the multi-view analysis yielded dramatic improvements (F1 scores ranging from 0.857 to 0.947). Moreover, the McNemar test confirmed that pipelines with a multi-view image assessment yields statistically significant classification improvements; however, the improvements this research observed between Pipeline A and B were not statistically significant. Thus, future research can explore the potential of LLM prompting in damage assessment. The practical contribution is an immediately deployable, flexible, and interpretable workflow that bypasses the need for supervised training, significantly accelerating triage and prioritization for disaster response practitioners.

Keywords: Wildfire Damage Assessment; Multi-view Ground-level Imagery; Vision–Language Models; Zero-shot Training-free Classification; Rapid Preliminary Damage Assessment

1. Introduction

The trajectory of recent wildfire seasons is alarming, evolving from natural ecological events into uncontrollable urban conflagrations that devastate the built environment (Dennison, Brewer, Arnold, 2014; Mahmoud & Chulahwat, 2018). Events such as the 2023 Lahaina disaster—the deadliest in Hawaii's history, claiming 102 lives and inflicting \$5.5 billion in damages (Insurance Institute for Business and Home Safety, 2024) —and Canada's unprecedented 2023 season, which burned 18.5 million hectares (Erni et al., 2024), underscore this escalating crisis. This threat is further exemplified by the January 2025 Eaton and Palisades fires in Los Angeles

County, which destroyed roughly 16,000 structures. As urbanization expands deeper into the Wildland–Urban Interface (WUI) (Mahmoud, 2024; Taccaliti et al., 2023), the frequency and scale of destruction are increasing globally (Ahmed et al., 2018; Chas-Amil et al., 2012; Chen & McAneney, 2004; Salvati, 2014; Sarricolea et al., 2020). Yet the critical process of post-fire damage assessment—essential for allocating aid and initiating recovery—remains a significant bottleneck.

Post-fire damage assessment provides information critical to priority allocation of proper resources to those most in need and provides appropriate aid to the local community. In the United States, governmental agencies charged with disaster response, such as the Federal Emergency Management Agency (FEMA), are responsible for such damage assessments (Luo & Lian, 2024). In current practice, a preliminary damage assessment (PDA) is conducted by a group of trained individuals to inspect the physical damage of the affected residential homes, despite accessibility issues with buildings or residences. There are also concerns about the inspectors' safety. Moreover, the volume of damaged homes could overwhelm the PDA teams (Luo & Lian, 2024). The use of unmanned aerial vehicles (drones) to gather aerial imagery has been integrated into the PDA process. To process these images, computer vision models are developed but are used by FEMA mainly for prioritizing the deployment of in-person damage assessors, rather than being used for damage assessments (Luo & Lian, 2024). Moreover, aerial imagery for damage assessment has several limitations. Structures may be obstructed by clouds or smoke, especially in wildfire situations. Processing the images requires significant computational and storage capabilities. Finally, aerial imagery often lacks the resolution required to assess individual structures. These limitations motivate this research to assess the potential language models, both Vision Language Models (VLMs) and Large Language Models (LLMs), for assessing ground-level images.

The current landscape of post-wildfire (PDA) is constrained by significant operational bottlenecks. While remote sensing and aerial imagery provide high-level overviews, they frequently fail to deliver the granular detail required for accurate, structure-level assessments due to obstructions like smoke or vegetation canopy. Consequently, the reliance on manual, in-person inspections persists—an approach that is resource-intensive, slow, and exposes personnel to hazardous environments. Although recent research has explored ground-level images (GLIs) as an alternative, the prevailing methodologies utilize supervised deep learning models, such as convolutional neural networks (CNNs) or vision transformers (ViTs) (Luo & Lian, 2024; Yang et al., 2025). These models are inherently data-hungry, demanding large labeled datasets that are impractical to generate rapidly in the chaotic aftermath of a disaster, thus failing to accelerate the assessment timeline when speed is most critical.

To address this gap, the objective of this research is to directly address the critical need for rapid and granular post-wildfire damage assessment, circumventing the limitations of manual inspections and the data dependency of traditional computer vision models. We propose a novel, zero-shot workflow utilizing pre-trained VLMs to analyze GLIs. The study specifically targets a significant gap in the literature: the persistent inaccuracy in classifying nuanced damage (the *affected* category). To overcome this, our methodology is designed to synthesize

multi-view perspectives, providing a holistic assessment beyond the front façade. Furthermore, we systematically evaluate the contribution of integrating domain-specific reasoning by comparing a VLM (Pipeline A) against a pipeline incorporating structured LLM prompts of wildfire damage indicators (Pipeline B). The rationale is to establish an accurate, interpretable, and immediately deployable framework that significantly accelerates the preliminary damage assessment process.

The remainder of the paper introduces a training-free, multi-view workflow that uses VLMs and LLMs for rapid wildfire damage assessment at the parcel level using GLIs. Unlike existing approaches that rely on satellite data or require extensive annotated datasets and complex preprocessing for supervised learning, our method can be deployed immediately in the aftermath of a wildfire event. The system leverages a pre-trained VLM (GPT-4o) combined with a streamlined library of binary damage indicators that guide the reasoning process and ensure output auditability. We evaluate two approaches: a zero-shot VLM baseline (Pipeline A) and a two-stage, indicator-guided variant (Pipeline B). Both pipelines explicitly support multiple views per household, addressing a critical practical requirement since façade images frequently fail to capture damage to the side or rear portions of structures. We validated the framework using two 500-sample case studies from the Eaton and Palisades fires of January 2025, drawing data from California's Damage Inspection (DINS) records. The methodology can be readily adapted to other natural hazards by modifying the indicator set. The results show that our approach achieves substantial performance improvements in the most challenging assessment category—the *affected* class—by effectively synthesizing multi-view evidence into consistent, reliable classifications across different events and pipeline configurations. From an operational perspective, this methodology addresses fundamental limitations of aerial imagery, including occlusion and insufficient parcel-level detail, while acknowledging that preliminary damage assessments remain resource-intensive. The framework provides emergency management practitioners with an immediately deployable, interpretable, and adaptable tool that can significantly accelerate post-fire triage and optimize resource allocation decisions.

1.1 Literature review

The literature review below is organized as follows: Section 1.1.1 examines how satellite imagery methods have been applied for wildfire damage assessment. Then section 1.1.2 examines the value of adding GLI data to damage assessment in both a flood and wildfire domain. Section 1.1.3 examines the application of computer vision language models.

1.1.1 Wildfire Damage Assessment via Satellite imagery

Damage assessment is a crucial component of post-wildfire disaster management, providing insights into the severity and spatial extent of destruction. Traditional methods have relied on remote sensing and satellite imagery, as these technologies enable decision makers to prioritize interventions, allocate resources, and plan for long-term recovery. Wheeler and Karimi (2020) trained a ResNet model on satellite imagery dataset that contained information on building damage after multiple natural hazards, such as a wildfire or flood (Wheeler & Karimi, 2020). Their model achieved an F1 score of 0.868. Galanis et al. (2021) used a ResNet18 model specifically to classify buildings as fully, partially, or non-damaged by training the model on post-

fire satellite images (Galanis et al., 2021). The researchers trained a ResNet18 model on post-wildfire satellite images, achieving 92% and 98% accuracy on test sets for their damage classification. These models provided insight on proper resource allocation post-event but required large amounts of training data and manual labeling. To mitigate this limitation, post-event reports integrate geospatial layers, semantic inference, and socio-economic overlays to provide actionable insights. Xie et al. (2020) used satellite radar imagery for damage assessment by applying machine learning to radar images which can visualize damages through smokes and clouds (Xie et al., 2020). Lee et al. (2020) uses a semi-supervised workflow that allows their model to be trained on a small amount of labeled data with a large amount of unlabeled data and found this performance to be similar to methods that were fully supervised (Lee et al., 2020).

Despite efforts to mitigate the limitations of satellite imagery, damaged structures from these images may still be obstructed by smoke clouds or large vegetation, unlike ground level-images, thus hindering interpretation. Moreover, processing data for aerial images requires significant computing power and adequate data storage. Therefore, computation-efficient methods are critical to serve the need for tools that can process complex datasets for rapid damage assessment. For these reasons, there is a shift in this research field that endeavors to better understand how non-satellite imagery data could be utilized in the context of damage assessment.

1.1.2 Ground-level images for damage assessment

GLIs can gather more information about household vulnerability than satellite imagery, improving damage assessment for researchers, practitioners, and city managers. For example, Nia and Mori used a CNN-based model trained on a small, manually curated GLI dataset to categorize buildings (ranging from no damage to severe damage). Their model achieved a 90% accuracy for the Ecuador and Nepal earthquake, as well as a 76% accuracy for Hurricanes Ruby and Matthew (Nia & Mori, 2017). Zhai and Peng applied a CNN to Google Street View (GSV) images to assess ground-level damage after Hurricane Michael struck Mexico Beach in Florida. Their model provided better insights compared to remote sensing images on household vulnerability by capturing damage to exterior walls, windows doors and facades (Zhai & Peng, 2020). Lou and Lian provided a ViT model to improve damage classification in a wildfire domain. They applied transfer learning to train a ViT model on 18,000 ground-level images of homes with damage severity labels assessed by damage inspectors during the 2020–2022 California wildfires. Their model achieved an F1 score of 0.73 for affected households, 0.99 for destroyed households, and 0.95 for no-damage households.

GLIs also help assess what household characteristics could make the property prone to a natural hazard. In the flood domain, the lowest floor elevation (LFE) is a key characteristic that can be determined from GLIs to better inform practitioners on the vulnerability of a household. Gao et. al (2023) used a deep learning computer vision model, YOLO-v5, to detect front doors to calculate the LFE of a household from GSV imagery by using a rectangular bounding box (Gao et al., 2024). Similarly, Ho et al. (2024) proposed a computer vision model, ELEV-VISION which uses a different bounding box (Ho, Lee, et al., 2024). These methods allowed researchers to better detect front doors and the height difference from the street and lowest floor. These

household elevation data, validated from ground truth elevation data by (Diaz et al., 2022) showed no statistical difference. To demonstrate the potential of GSV imagery to improve flood predictions, Esparza et al. (2025) used the household elevations from ELEV-VISION in flood depth-damage curves. They found statistical significance with both flood depth data and insurance claims (Esparza et al., 2025). These works show the potential that ground level imagery has to be used in damage assessment by discovering key household features that could cause vulnerability.

To advance the potential that GLIs have in rapid damage assessment, the methodological contribution of the research is integrating these images in a vision language model (VLM). The current literature of VLMs is explored in section 1.2.3 and can be further enhanced by using LLM prompting techniques to guide the VLM for enhanced damage assessment.

1.1.3 Vision language models for post disaster assessment

The applications of vision language models in natural hazard research have opened opportunities for damage assessment; however, VLM in damage assessment has been historically constrained by the scarcity of large-scale, annotated image-text datasets. Several studies to overcome this limitation by developing novel datasets and training frameworks. For instance, Wang et al. (2023) developed a large-scale remote sensing vision-language dataset using Google Earth imagery and OpenStreetMap data. Models trained on their dataset demonstrated an increased accuracy of 6.2% in zero-shot scene classification compared to models that are not trained on their dataset (W. Wang et al., 2023). Junjue Wang et al. (2023) curated a multi-modal dataset for natural hazard analysis, encompassing 36 events related to floods, wildfires, and earthquakes (J. Wang et al., n.d.). This specialized dataset not only aids emergency response planning but also improved model accuracy by 10.4% over baselines. Mall et al. (2024) introduced a framework that leverages paired satellite and ground-level imagery to train VLMs without explicit textual annotations, showing that this approach outperforms traditional baseline models (Mall et al., 2024).

VLMs have also been used in damage assessment. For example, Ho et. al (2024) built upon their previous work of the ELEV-VISION model by adding text-prompted image segmentation, improving their previous results by obtaining a 75.63 Intersection over union segmentation task. The integration significantly enhanced the availability of LFE estimation from 33% of properties to 56%, covering nearly all houses (98.71%) where the front door was visible, while maintaining comparable accuracy to baseline models (Ho, Li, et al., 2024). A multimodal model that processes both images and text-based tabular data simultaneously shows potential to improve prediction of houses burning during a wildfire event (Iván Higuera-Mendieta, Jeff Wen, 2023). The research used datasets with pre-fire aerial imagery and tabular data on household characteristics, weather features, and a fire hazard rating. The tabular data was converted into descriptive text prompts and assessed in language models, such as RoBERTa and GPT-2. The image dataset was processed with a ViT and ResNet50 model. A multimodal approach with the ViT and RoBERTa models achieved the highest F1-score of 0.77 compared to models that were trained only on vision and text.

The novelty of this research is to establish a methodological framework for practitioners to implement after a wildfire event to significantly enhance damage assessment. This is accomplished by using pre-trained VLM and LLM tools to classify the damage extent of households based on GLIs.

1.2 Study objective

This study proposes two pipelines to explore how language models can enhance in wildfire damage classification. There is a noticeable gap in the literature as current models struggle to properly classify households where the damage is not in the front façade (Luo & Lian, 2024). By utilizing a VLM pipeline (Pipeline A), and VLM+LLM pipeline (Pipeline B), this research examines the extent that language models can improve damage classification after a wildfire event. This is possible by the pipelines being able to process multiple images for a single household by computationally treating each view as an independent embedded image which retains the properties that the images contain. Both pipelines are used to process only the front of the household and then process all associated images of the household. The first objective of this research is to determine the extent that language models can enhance wildfire damage assessment. This is observed by comparing the results of the single image assessment and multi-view assessment. The second objective is to determine the potential of LLM prompting techniques have for classification enhancement. This is observed by comparing the results of Pipeline A and Pipeline B. These two objectives will assesses the potential of language models to provide practitioners with a comprehensive workflow that can be used post-fire to aid PDA by enhancing classification accuracy and speed.

2. Methodology

Section 2.1 will examine the study area and collected data. Section 2.2 will explain the construction of the proposed pipelines. Section 2.3 will provide an overview on the McNemar test and classification metrics this research uses.

2.1 Study area and data

During the month of January 2025, Los Angeles County experienced two catastrophic firestorms, the Palisades and Eaton fires. These fires evolved from wildland fires into uncontrollable urban fires and destroyed roughly 16,000 structures as well as claimed 30 lives. The conflagrations of these fires made both events the second (Eaton) and third (Palisades) most destructive fires in California's history. This was due to a combination of extreme weather conditions—such as droughts—before the fire; dense community construction (separation of structures were as low as 8 to 20 feet); and the on-going urban development in wildland areas (Eaton, 2025).

The Palisades and Eaton damage data comes from the California Natural Resource Agency Damage Inspection Program (DINS) database. The database contains records of wildland fires dating back to 2013 and documents the damage of structures in affected areas. The Palisades fire impacted 12,000 structures, and the Eaton fire, 18,000. The structures' damage classification are as follows: *no damage*, *minor*, *affected*, *major*, and *destroyed*.

Pre-processing began with calculating the cosine similarity score with OpenAI's CLIP model for the entire dataset of Palisades and Eaton. The model will use an encoder to project the image inputs into an embedded vector space. Then, the cosine of the feature vectors are computed. This output is a measure of similarity between images based on high-dimensional feature representation. The equation for the cosine similarity score is shown below.

$$\text{Cosine Similarity } (x, y) = \frac{x \cdot y}{\|x\| \|y\|} \quad (1)$$

In the above equation, x is the *affected* category while y would be either minor or major category. The dot product of the vectorized images is taken and it is divided by the product of the magnitude of these categories. A higher score indicates that the categories show similarities in these images.

An additional pre-processing step involved taking 500 random samples for each study area. Since the aggregation was feasible for the whole dataset, no cosine similarity scores were computed on the samples. Taking a smaller sample set was necessary due to computational and monetary limitations of running the pre-trained model. Additionally, the results would only marginally improve since the model is pre-trained despite more computational and monetary resources. Figure 1 shows the study areas and sample data for Palisades and Eaton fires.

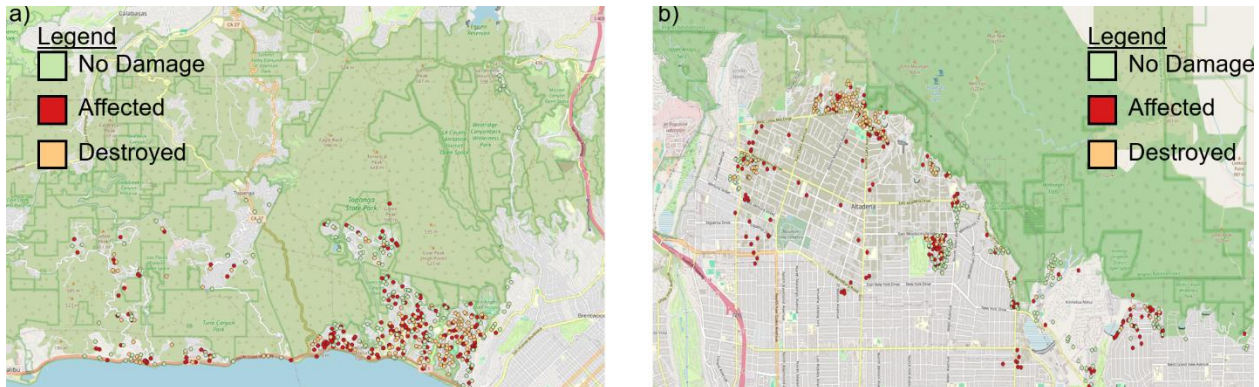


Figure 1: Study area of 500 samples in (a) Palisades Fire and (b) Eaton Fire.

2.2 Methodological Framework

This study establishes a workflow that is capable of processing multiple images for a single household in wildfire damage assessment. This is achieved by using the capabilities of a VLM to process a list of embedded images in a single for loop. Additionally, this research explores the potential that LLM prompting techniques have for enhancing damage assessment. To accomplish these objectives, the research uses the pre-trained GPT-4o VLM and LLM models to build two pipelines. Both proposed pipelines are used to analyze a single front view image of a household, and the other perspective of a house when multiple images are available.

Figure 2 shows the workflow of both proposed pipelines. Pipeline A only uses the VLM model, after the images are passed in base64 format, and is tasked to classify the images as *no damage*, *affected*, or *destroyed*. Pipeline B is a modified version of Pipeline A, where the VLM is

now tasked to assess damage indicators from the encoded image. These will output true/false values that are then fed into the LLM to make a classification based on the binary results from the VLM and encoded image. Both proposed pipelines are used to analyze a single front view image of a household, and the other perspective of a house when multiple images are available. Section 2.2.1 and section 2.2.2 outline the details of Pipeline A and Pipeline B respectively.

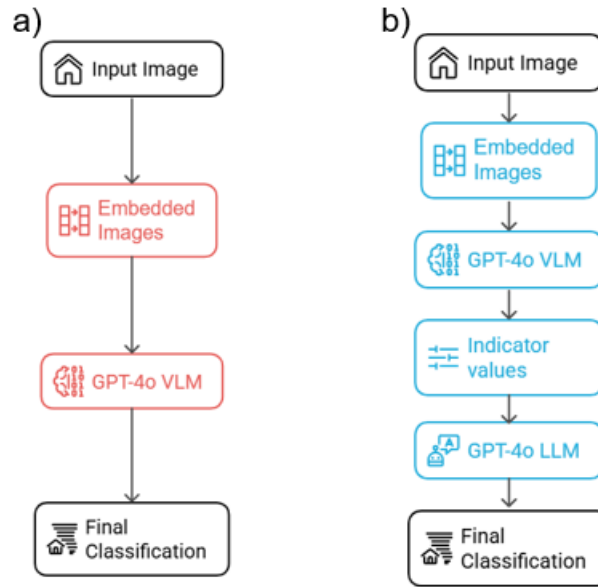


Figure 2: Methodological framework. (a) Pipeline A is a VLM pipeline that is prompted to classify the damage based on the image. (b) Pipeline B uses the VLM to assess damage indicators based on the embedded images. These will be true/false values for the LLM to make a damage classification based on both the embedded image and indicators from the VLM.

2.2.1 *Exploring the potential of Vision Language Modeling in damage assessment*

For Pipeline A, the image(s) are directly provided to the model, which classifies the wildfire damage into the no damage, affected, and destroyed categories without providing further context. Thus, the pipeline lacks an intermediate step for visual parameters. This gives the model flexibility to classify a house without abiding by the cues given to it; however, this simplicity also limits the extent to which data can be interpreted and the confidence of along with domain-specific analysis for these images. This research compares the output of this pipeline for both the single view of the household and multi-view of the household for both study areas. The VLM is capable of processing multiple images for a single household through its ability to take multiple embedded images as a list. For example, a household with three images will have three respective embedding's that will be aggregated into a list. The single view and multi-view approach are then compared to determine the extent of improvement that assessing multiple images of a single household can provide. Algorithm 1 presents the pseudo code for this pipeline.

ALGORITHM 1: Pipeline A

Input : Image set $I = \{I_1, I_2, \dots, I_n\}$, text prompt T , vision-language model $VLM \in \{\text{"GPT-4o"}\}$

Output: Damage label $L \in \{\text{'Affected'}, \text{'No Damage'}, \text{'Destroyed'}\}$

```
1 For each house:  
2             Prompt T ←  
3                 "You are an expert in post wildfire disaster building damage assessment.  
4                 Given a building's image, decide if it is 'Affected', 'No Damage', or 'Destroyed'.  
5                 Just output the label of the classification."  
6  
7 { E1, E2, E3} ← Encode up to 3 images for the house in base64 format: {I1, I2, I3}  
8  
9 Response R ← VLM(T, { E1, E2, E3 })  
10  
11 L ← R.label // Model outputs one label based on input images and prompt  
12  
13 end
```

2.2.2 Including Large Language Modeling into Wildfire Damage Assessment

Pipeline B, built by augmenting the Pipeline A, includes an intermediate output from the VLM. This two-stage pipeline benefits from its reasoning ability based on visual cues identified by the provided prompt indicators. First, the VLM processes the image(s) of the houses and outputs a set of structured indicators along with their corresponding true or false values. Then, the outputs are passed to an LLM, which integrates these cues with the contextual prompt to determine the label for the houses. The indicators this research selected are based on literature and are explained in the appendix. Pipeline B is applied to both the single view image and multi-view image test. The results of this test are compared to each other to accomplish the first research objective. To accomplish the second objective, these results are also compared to the respective classifications of Pipeline A to determine the extent that LLM prompting can improve damage assessment.

Algorithm 2: Pipeline B

Input: Image set $I = \{I_1, I_2, \dots, I_n\}$, structured text prompt T_1 , VLM $\in \{\text{"GPT-4o"}\}$, indicator-based prompt T_2 , LLM $\in \{\text{"GPT-4o"}\}$

Output: Damage label $L \in \{\text{'Affected', 'No Damage', 'Destroyed'}\}$

```
1  For each house:  
2      VLM Indicator prompt  $T_1 \leftarrow$   
3      "Analyze the image and answer with a JSON object in the following format:  
4      {  
5          'is the house destroyed': true/false,  
6          'is the structure damaged': true/false,  
7          'is the glass or windows broken': true/false,  
8          'is the furniture burnt': true/false,  
9          'are there burn marks on the structure': true/false,  
10         'is the vegetation around burnt': true/false  
11     }  
12     Only output the JSON object, nothing else."  
13  
14     {  $E_1, E_2, E_3 \leftarrow$  Encode up to 3 images for the house in base64 format:  $\{I_1, I_2, I_3\}$   
15     Indicators JSON  $V \leftarrow$  VLM( $T_1, \{E_1, E_2, E_3\}$ )  
16  
17     LLM prompt  $T_2 \leftarrow$   
18     "You are an expert in post wildfire disaster building damage assessment.  
19     Given a building's attributes in JSON, decide if it is 'Affected', 'No Damage', or 'Destroyed'.  
20     If the attribute says destroyed is true, then output 'Destroyed'.  
21     If any one of the other attributes are true, then output 'Affected'.  
22     If none of the attributes are true, then output 'No Damage'.  
23     Now, decide for this building:  
24     {Indicators JSON  $V\}$   
25     Output only one word: 'Affected', 'No Damage', or 'Destroyed'. "  
26  
27     Response  $R \leftarrow$  LLM( $T_2$ )  
28  
29      $L \leftarrow R.\text{label}$  // Model outputs one label based on indicators JSON  
30  
31 end
```

2.3 Statistical testing and classification parameters

This research uses precision (equation 2), recall (equation 3) and the F1 score (equation 4) score to evaluate the classification results of each pipeline.

$$Precision (P) = \frac{TP}{TP+FP} \quad (2)$$

$$Recall (R) = \frac{TP}{TP+FN} \quad (3)$$

$$F1\ score = 2 * \frac{P*R}{P+R} \quad (4)$$

These metrics are the standard criterion for evaluating classification problems (Yang et al., 2025). TP refers to a true positive classification which is an image that was correctly classified into its respective damage level. FP refers to a false positive and occurs when the model incorrectly assigns an image into a class. FN is a false negative and occurs when the model overlooks class features of an image. The F1 score is calculated as the harmonic mean of P and R which provides a balanced metric to evaluate the model's classification performance. This metric will be used when discussing the results of the pipelines.

To statistically compare the performance of different modeling approaches, we employed McNemar's test. This test is suitable for analyzing paired categorical data, allowing us to evaluate the marginal homogeneity between two models' predictions on the same dataset. A two by two contingency table was constructed for each comparison, tabulating the instances where both models were correct, both were incorrect, and where they disagreed. The test focuses specifically on the asymmetry of the disagreement counts. A statistically significant result ($p < 0.05$) indicates that the two models have different error rates. We conducted this test for three distinct cases:

Case 1: single-view vs. multi-view results within Pipeline A to evaluate the impact of a multi-view image assessment.

Case 2: single-view vs. multi-view assessment within Pipeline B to evaluate the impact of a multi-view image assessment.

Case 3: multi-view assessment of Pipeline A vs. Pipeline B to evaluate the impact of LLM prompting.

The McNemar's coefficient is calculated by equation 5, where b and c are the classification results for the pipelines.

$$X^2 = \frac{(|b-c|-1)^2}{b+c} \quad (5)$$

A high X^2 value allows the research to reject the null hypothesis. In this application, the null hypothesis for case 1 and case 2 would be that there is no statistical significant difference in the error rates between the single view and multi-view assessment; therefore, both image assessments preform equally well. By rejecting the null hypothesis for these two cases, the potential improvement between a single view and multi-view assessment does not randomly occur. For case 3, similar logic applies except, this will determine if any improvement that LLM prompting can provide for the multi-view image assessment occurs randomly.

3. Results

To examine the extent to which the proposed methodology can improve wildfire damage assessment, section 3.1 will provide an overview of the cosine similarity score to assist with model classification and the computational resources this workflow requires. Section 3.2 examines the classification metrics of single front-view GLI for Palisades and Eaton among both pipelines. Section 3.3 applies both pipelines on multiple views of the households when applicable. The classification results from section 3.2 and 3.3 will be statistically compared through the McNemar test in section 3.4. Finally, a visual analysis is performed to complement the results of both pipelines in section 3.5.

3.1 Data Contextualization

Table 1 compares the number of households in each category for the original dataset and the sampled dataset for both study areas. Few households in either the total or sample datasets in both study areas are classified as sustaining *minor* or *major* damage. This classification prompted the need for the research to aggregate the data into the *affected* category similar to Lou and Lian (2024). To computationally validate this aggregation, the cosine similarity scores were calculated with OpenAI's CLIP model based on the encoded images.

Table 1: Number of households in each damage category

Category	Eaton Total Data	Eaton Sample Data	Palisades Total Data	Palisades Sample Data
No Damage	7,894	155	4,262	155
Affected	856	181	730	178
Minor	148	6	171	8
Major	70	3	72	4
Destroyed	9,413	155	6,835	155

Table 2 shows the cosine similarity score for both study areas. The *affected* versus *minor* (Eaton: 0.794; Palisades: 0.730) and *affected* versus *major* (Eaton: 0.766; Palisades: 0.728) categories are rather high. Due to the small sample size of *affected*, *minor*, and *major* along with the high cosine similarity score, these categories are grouped together as affected. This approach was also used by Lou and Lian (Luo & Lian, 2024) on a similar damage dataset for California Wildfires that occurred during 2020-2022.

Table 2: Cosine Similarity Score

Category	Eaton Cosine Score	Palisades Cosine Score
Affected vs minor	0.794	0.730
Affected vs major	0.766	0.728
Within affected	0.797	0.730
Within destroyed	0.861	0.753
within no damage	0.797	0.727

The research took 500 random samples because of monetary and computational constraints. The usage of VLM and LLM requires monetary resources based on tokenization, which is the process of transforming images into compressed representative units that can be processed by these models. The number of tokens used depends on the length and complexity of both the input and output of the model. Each experiment had 500 samples, with some samples containing more than one image. Whenever an API call is made to the model, both the input prompt in the form of text and images, and the output generated for the classification contribute towards the count of total tokens used. To manage token usage and ensure output consistency, the *max_tokens* hyperparameter, which sets the maximum length of the generated output, and the *temperature* hyperparameter, which controls the randomness of the output, were controlled for each pipeline stage. The *max_tokens* parameter was matched to the expected response length—low for simple classifications and high for structured outputs. Concurrently, the *temperature* was set low (0.0-0.2) for the deterministic tasks in Pipeline B and moderately (0.5) for the classification task in Pipeline A to adapt the models for their specific roles. Table 3 presents a summary of the computational resources for each pipeline.

Table 3. Summary of the computational resources of the APIs for the VLM and LLM

Tokens per 10 samples	Multiple images (2)	Multiple images (3)	Ground level images	Multiple images (2)	Multiple images (3)	Ground level images
VLM input tokens	9,320	15,440	5,240	9,770	15,890	5,690
VLM output tokens	14	15	18	660	660	608
LLM input tokens	0	0	0	1,930	1,930	1,904
LLM output tokens	0	0	0	11	12	18
Total price for 1 sample (\$)	0.002344	0.003875	0.001328	0.003596	0.005127	0.0025245
Total price for 10 samples (\$)	0.02344	0.03875	0.01328	0.03596	0.05127	0.025245

In Pipeline A, the tokens are counted for the single stage process where the VLM receives image(s) as input and directly outputs the classification. In Pipeline B, tokens are counted separately for both the stages (VLM and LLM) where the VLM receives image(s) along with a guided prompt and the LLM inputs the computed indicator values along with the context. This token counting is done for both the single and multiple images scenarios for each pipeline. For this purpose of cost calculation, we sampled 10 records under each experimental scenario, and measured the input and output token count for each component in the pipelines. The operational cost for each pipeline was calculated based on per-token pricing, with input tokens at $\$ 2.0 \times 10^{-6}$ and output tokens at $\$ 1.0 \times 10^{-5}$. For Pipeline A, the cost per sample ranged from approximately \$0.00133 for a single image to \$0.00388 for three images. In contrast, Pipeline B consistently incurred higher costs, ranging from \$0.00252 for a single image to \$0.00513 for three images. These costs are relatively cheap making this method monetarily feasible to implement after a natural hazard occurs, but users should be mindful of these resources.

3.2 Application of language models in a single view front image analysis for damage assessment

The single front view GLIs are assessed with both pipelines in each study. Figure 3 shows the confusion matrix for Eaton and Palisades. In all four-confusion matrixes, the prediction for *destroyed* and *no damage* were generally classified correctly; however, the *affected* category had the most misclassifications, as a majority of these images were classified as *no damage*.

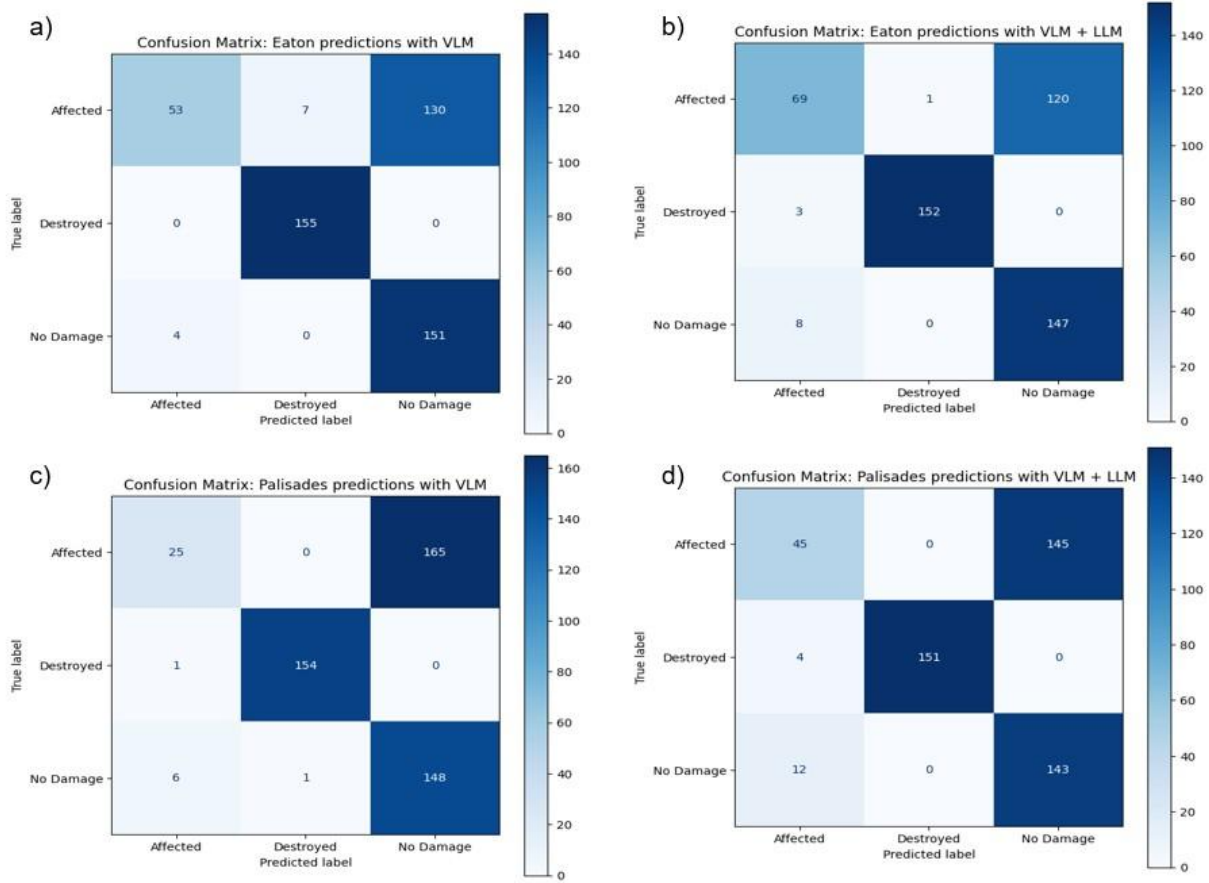


Figure 3: Confusion matrix for the single view test for Eaton with Pipeline A (3a), and Pipeline B (3b); Palisades with Pipeline A (3c) and Pipeline B (3d).

Table 4 shows the percentage of correctly classified results. These results show that the *affected* category had the lowest percentage of correctly classified households for both study areas. Moreover, Pipeline B has a slightly higher percentage of correctly classified households for the *affected* category compared to Pipeline A. This suggests that LLM prompts could have the potential to enhance damage classification. Especially when it is rather difficult for a computer model to determine damage, as the prompts can guide the models decision making. While the LLM based prompts did improve the classification for *affected* the *no damage* and *destroyed* category did have a slight reduction in classification, signaling a trade off with an LLM based approach. Moreover, future research can explore the potential of LLM prompts to finetune prompting techniques to enhance damage classification and mitigate tradeoff. To expand on these results the classification metrics are calculated.

Table 4: Percentage of correctly classified households

	Eaton Pipeline A (Figure 3a)	Eaton Pipeline B (Figure 3b)	Palisades Pipeline A (Figure 3c)	Palisades Pipeline B (Figure 3d)
No Damage	97.4% (151/155)	94.8% (147/155)	95.5% (148/155)	92.3% (143/155)
Affected	27.9% (53/190)	36.3% (69/190)	13.2% (25/190)	23.7% (45/190)
Destroyed	100% (155/155)	98.1% (152/155)	99.4% (154/155)	97.4% (151/155)

Table 5 shows the classification metrics of both pipelines for each study area. The F1 scores are used for comparison; however, precision and recall are calculated and presented for transparency. The *affected* category had the lowest F1 scores for both pipelines in each study area, ranging from (0.225 to 0.511). This suggests the need for a workflow that can process multiple images for the same household as the damage could have occurred at another location of the household. These findings are similar to Lou and Lian, as they found their *affected* category predictions from the trained ViT model to be the lowest of their three classification categories (Luo & Lian, 2024).

Table 5: Classification Metrics for Single Front View Images

Metrics	Eaton Pipeline A	Eaton Pipeline B	Palisades Pipeline A	Palisades Pipeline B
Accuracy	0.718	0.736	0.654	0.678
Micro-Average F1 Score	0.718	0.736	0.654	0.678
Macro-Average F1 Score	0.700	0.732	0.617	0.663
No Damage				
Precision	0.537	0.551	0.473	0.497
Recall	0.974	0.948	0.955	0.923
F1 Score	0.693	0.696	0.633	0.646
Affected				
Precision	0.930	0.863	0.781	0.738
Recall	0.279	0.363	0.132	0.237
F1 Score	0.429	0.511	0.225	0.359
Destroyed				
Precision	0.957	0.994	0.994	1.00
Recall	1.00	0.981	0.994	0.974
F1 Score	0.994	0.987	0.994	0.997

The main rationale why this research decided to use a pre-trained VLM model is to specifically better classify the *affected* category by processing multiple images for the same household. While a ViT can lead to higher F1 scores in some cases with a single image, training a model that can process multiple images is a rather cumbersome task. The input data would need to embed each image for the household, and then average the embeddings. This approach is not fully practical for practitioners to utilize when a pre-trained model like a VLM exists, as this is a

time intensive task that may miss key details from the image. Moreover, the VLM workflow provides the user flexibility with the integration of LLM prompts as they can adapt prompts based on their natural hazard situation.

3.3 Application of language models in a multi-view image analysis for damage assessments

The results from section 3.2. show the need to improve classification, specifically for the *affected* category. This research accomplishes this by using the same two pipelines and datasets but adding multiple views of houses when these views are present. Figure 4 shows the confusion matrix.

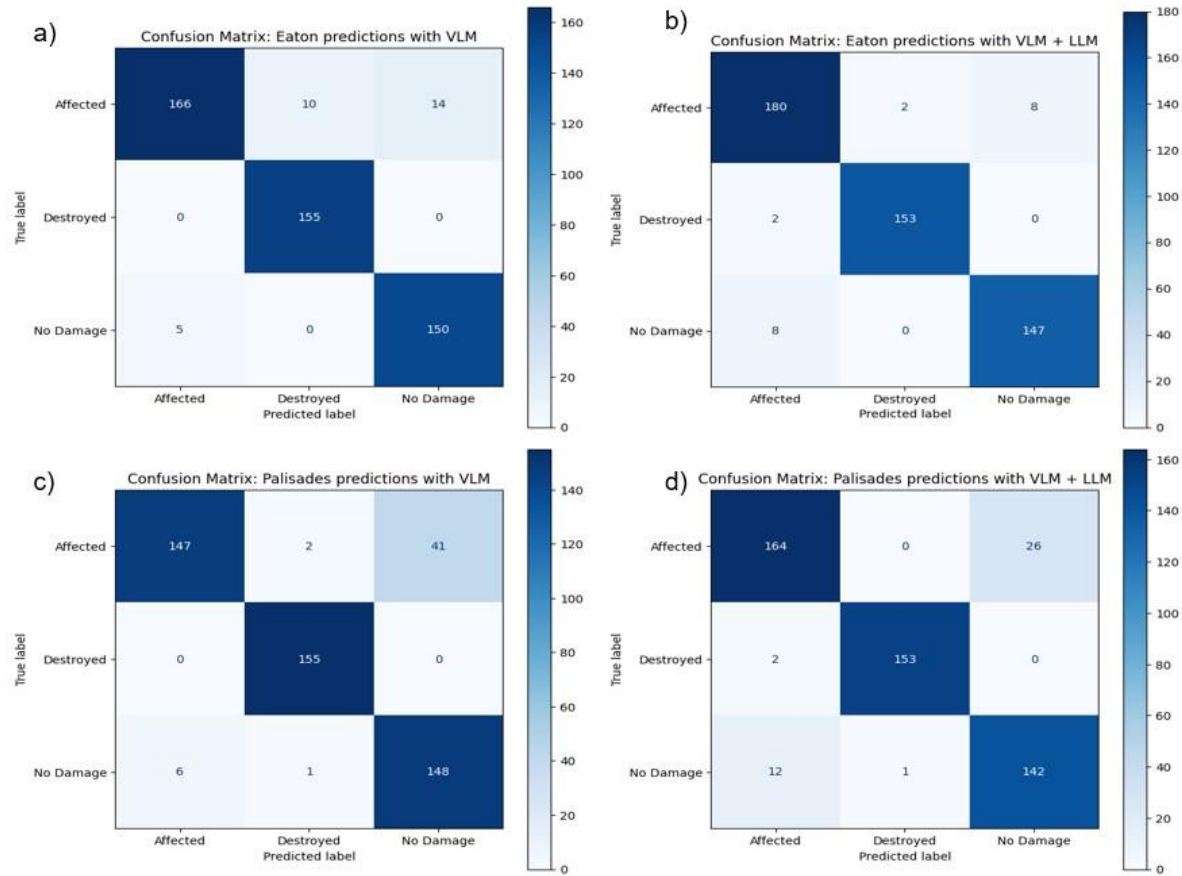


Figure 4: Confusion Matrix Confusion matrix for the multi-view test for Eaton with Pipeline A (4a), and Pipeline B (4b); Palisades with Pipeline A (4c) and Pipeline B (4d).

Table 6 shows the percentage of correctly classified households for the multi-image assessment. The value of language models in wildfire damage assessment is seen when comparing the results of table 6 with table 4 as more *affected* households are correctly classified when using multiple images for a single household. This shows promise for practitioners to adopt this workflow when assessing wildfire damage.

Table 6: Percentage of correctly classified households

	Eaton Pipeline A (Figure 4a)	Eaton Pipeline B (Figure 4b)	Palisades Pipeline A (Figure 4c)	Palisades Pipeline B (Figure 4d)
No Damage	96.8% (150/155)	94.8% (147/155)	95.5% (148/155)	91.6% (142/155)
Affected	87.4% (166/190)	94.7% (180/190)	77.4% (147/190)	95.5% (155/190)
Destroyed	100% (155/155)	98.7% (153/155)	95.5% (155/155)	98.7% (153/155)

Table 7 shows the classification metrics for both pipelines in each study area, when assessing multi-view images. The main finding from these results is that the *affected* category had a substantial increase in their F1 scores when compared to table 5. This suggest that multi-view image assessment is critical for damage classification as the model can better capture damage visuals. Moreover, the *destroyed* category results were largely unaffected by adding multi-view images as most households for this category had only one image. For *no damage*, this metric improved significantly as well mostly because the bulk of the misclassifications for affected, when examining the confusion matrix in figure 3, were allocated to the no damage category.

Table 7: Classification Metrics for multi-view Images

Metrics	Eaton Pipeline A	Eaton Pipeline B	Palisades Pipeline A	Palisades Pipeline B
Accuracy	0.942	0.960	0.900	0.960
Micro-Average	0.942	0.96	0.900	0.96
F1 Score				
Macro-Average	0.943	0.961	0.903	0.961
F1 Score				
No Damage Category				
Precision	0.915	0.948	0.783	0.845
Recall	0.977	0.948	0.955	0.916
F1 Score	0.940	0.948	0.861	0.879
Affected Category				
Precision	0.971	0.947	0.961	0.921
Recall	0.874	0.947	0.774	0.863
F1 Score	0.920	0.947	0.857	0.891
Destroyed Category				
Precision	0.939	0.987	0.981	0.994
Recall	1.00	0.987	1.00	0.987
F1 Score	0.967	0.987	0.990	0.990

An additional finding is that LLM prompts show some potential when enhancing damage assessment. Though these improvements are minor and could be as a result of the sample size, the value that LLM prompts have is the fact that it can give practitioners the flexibility to alter the prompts based on the type of natural hazard event or severity of the event (cite ali paper that he shared). Moreover, future research can enhance the LLM prompts with RAG concepts or adding relevant documents such as forensics reports or cost estimates to establish a novel knowledge base. To empirically test the enhancement of both the multi-view assessment and addition of LLM prompts, section 3.4 presents the results of the McNemar test.

Section 3.4 Statistical analysis how language models improve damage classification

The research performs the McNemar's test on three cases. Case 1 is a comparison of Pipeline A's single view and multi-view assessment. Case 2 is similar to case 1 but with the results of Pipeline B. Case 3 compares the multi-view results of Pipeline A and B to determine the extent that LLM prompting can improve classification. Table 8 shows the McNemar's coefficient and p-values for the three cases and presents the number of households that have multiple images for each damage category to contextualize the statistical results.

Table 8: The classification improvements VLMs and LLMs provide in damage assessment

Eaton			Palisades		
Case 1: McNemar's test for Pipeline A's single view and multi-view classification results					
No damage	Affected	Destroyed	No damage	Affected	Destroyed
111.08***	106.22***	1	118.20***	117.20***	1
Case 2: McNemar's test for Pipeline B's single view and multi-view classification results					
No damage	Affected	Destroyed	No damage	Affected	Destroyed
106.22***	108.47***	1	108.64***	111.63***	1
Case 3: McNemar's test on the multi-view results for Pipeline A and Pipeline B					
No damage	Affected	Destroyed	No damage	Affected	Destroyed
0.266	3.56	1	0.124	2.06	1
Number of households with multiple images					
No damage	Affected	Destroyed	No damage	Affected	Destroyed
3	175	6	11	190	8

p-value: * <0.01 ** 0.05 *** <0.0001

The table shows the no damage and *affected* category's classification improvements are statistically significant for case 1 and case 2. However, for case 3, the improvements were not statistically significant. For all three cases the *destroyed* category did not show any statistically significant improvement. There were 175 and 190 households with multiple images in Eaton and Palisades respectively. This is a contribution to the results of the McNemar's test. Most households that were *affected* were classified as *no damage* when using the single front façade images of the household (as shown in the confusion matrix in figure 3). When the multi-view assessment was conducted, the VLM workflow was capable of allocating most affected households to the correct category. While the *no damage* category had little households with multiple images, the improvement was statistically significant due to the correct classification of affected households. The front façade of a household who was *affected* by the wildfire had a similar façade as *no damage* households and not the destroyed households, as seen in the visual analysis in section 3.5. These results show that research objective 1 was accomplished as a VLM workflow improved wildfire damage classification especially in *affected* households due to its ability to process multiple embedded images while retaining the vectorization priorities of each image. The second research objective was not statistically significant but LLM prompting still is a valuable avenue for future research to explore as they can provide context to the image and enhance classification with other methods such as RAG.

To complement the results in table 8, figure 5 through figure 7 show a contingency matrix of each case for only the *no damage* and *affected* category in each study area. The additional number of households that the multi-view assessment was able to correctly classify for Pipeline A was 116 – 126 (as seen in the respective categories for figure 5) and 114 – 125 for Pipeline B (as seen in the respective categories for figure 6). Figure 7 shows that Pipeline B was only able to correctly classify 9 – 20 additional households compared to Pipeline A.

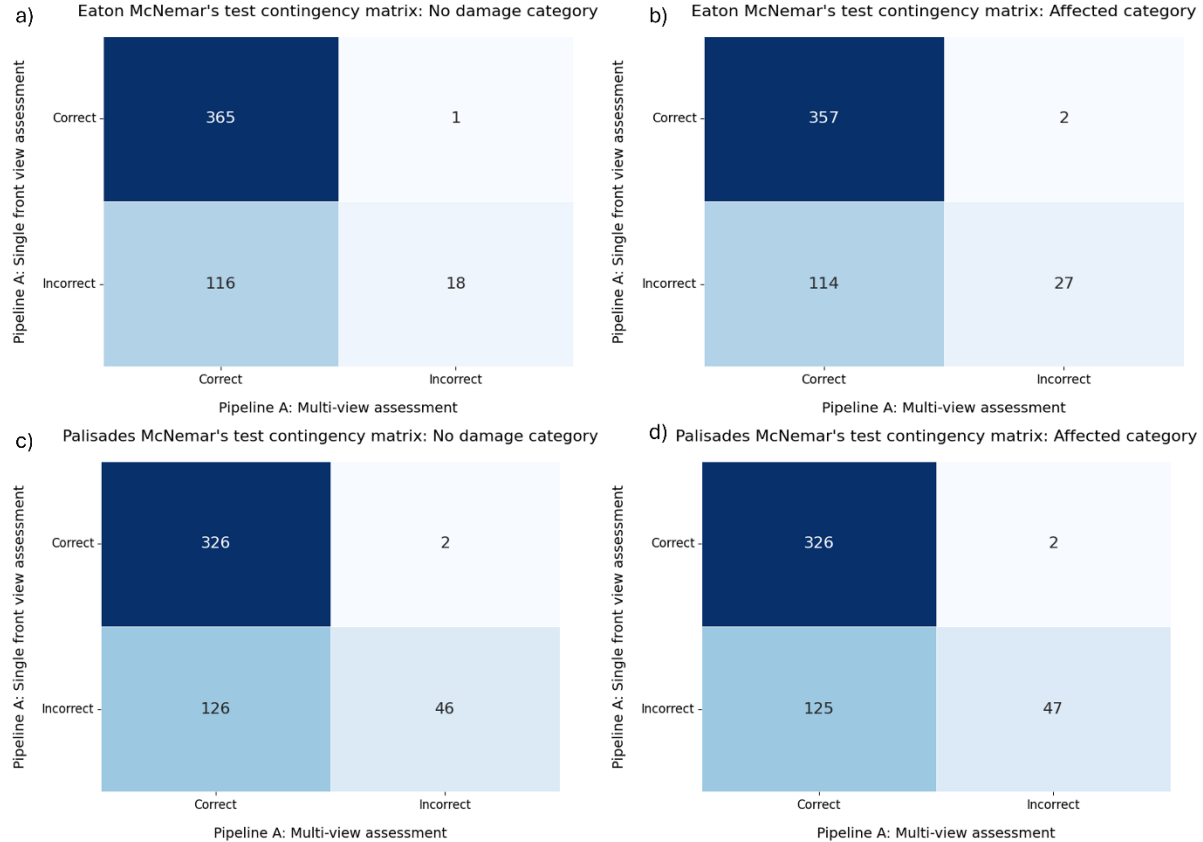


Figure 5: McNemar's test for comparing Pipeline A's single view (y axis) and Multi-view (x axis) classification results. The multi-view assessment had better classifications for No damage category in Eaton, by 116, and Palisades, by 126. The same can be seen for the Affected category in Eaton, 114 and Palisades, 125.

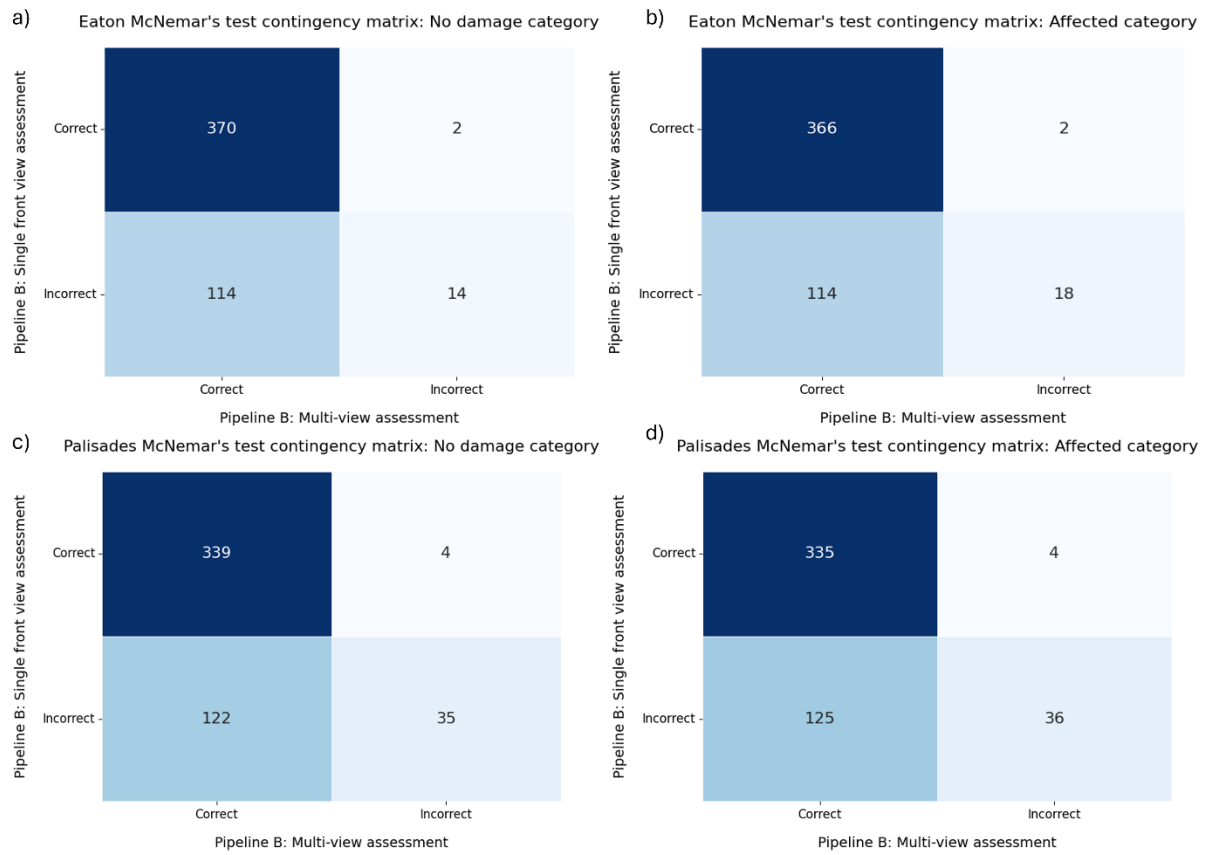


Figure 6: McNemar's test for comparing Pipeline B's single view (y axis) and Multi-view (x axis) classification results. The multi-view assessment had better classifications for No damage category in Eaton, by 114 , and Palisades, by 122. The same can be seen for the Affected category in Eaton, 114 and Palisades, 125.

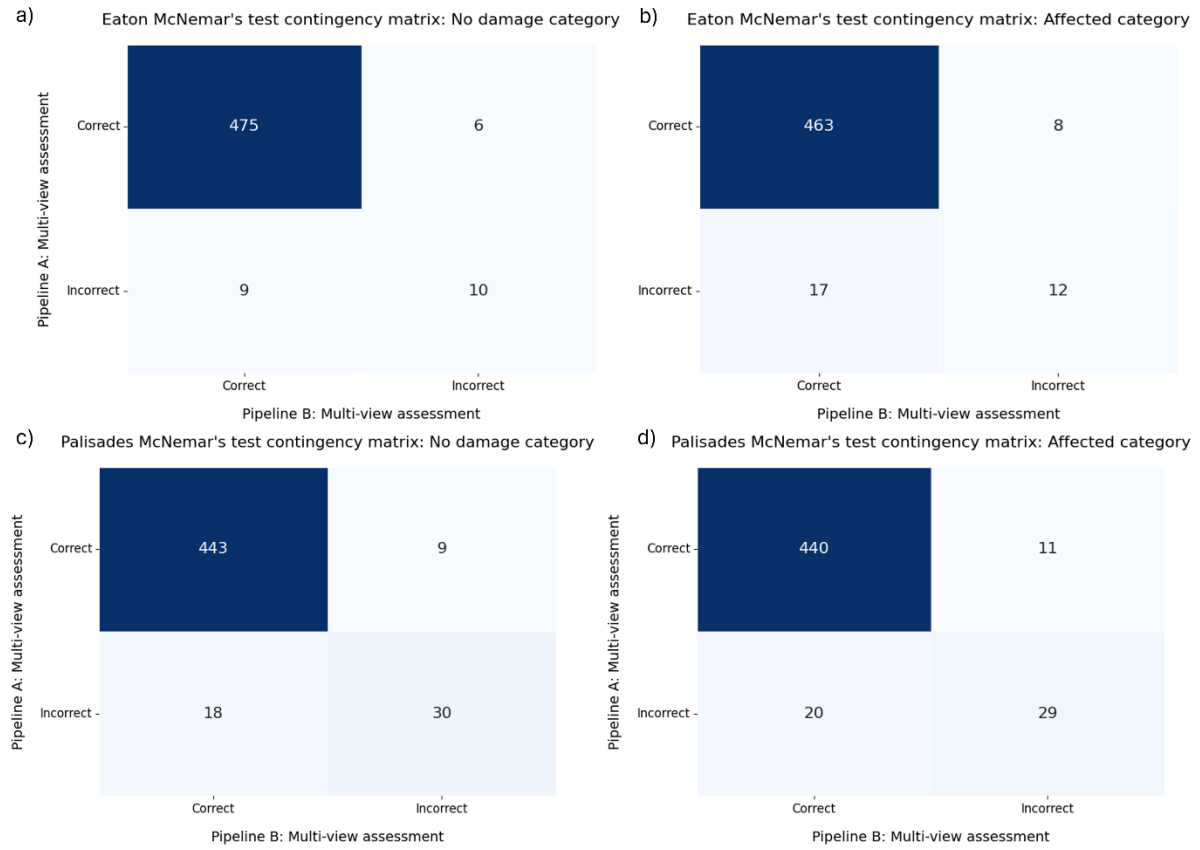


Figure 7: McNemar's test for comparing the multi-view assessment classifications for Pipeline A and Pipeline B. The improvements were not statistically significant as Pipeline B improved 7a by nine images, 7b by 17 images, 7c by 18 images, and 7d by 20 images.

These findings demonstrate the practicality of utilizing language models to enhance wildfire damage assessment. Specifically, VLMs capability of properly processing multiple images significantly improved the affected category which was a critical needed to this field (Luo & Lian, 2024). Moreover, the model is pre-trained which bypasses the need for complex data pre-processing, such as taking the average of embedded images, to accomplish a similar feature. Additionally, this workflow does not need any training or testing data and practitioners can use this workflow with a VLM instantly after a natural hazard strikes to enhance damage assessment. Another practical contribution is that Pipeline B shows potential to enhance classification results, with a slight cost increase, and provides practitioners flexibility to adjust the LLM prompts depending on the local community's needs, type of natural hazard, and location of the event.

3.5 A visual analysis on the VLM and LLM workflow

Pipeline B, with its marginally better results, was the test case for the visual analysis, using randomly selected samples for both the single-front view and multi-view. The first set of images were examples of Pipeline B's misclassification as shown in Figure 8. The model classified

these structures as affected. The structures, however, were clearly not livable; therefore, they were destroyed, according to the ground truth label. In all cases, the image has a standing structure which could be a cause for confusion for the model. Figure 9 (a–d) shows destroyed structures that were correctly classified in both single-front and multi-view. The model was able to pick up rubble in the background in Figure 9 (b). In contrast, in Figure 8, the destroyed structures were standing to some degree. This provides an opportunity to finetune LLM prompts to capture cases in which unlivable homes are still standing from the fire.

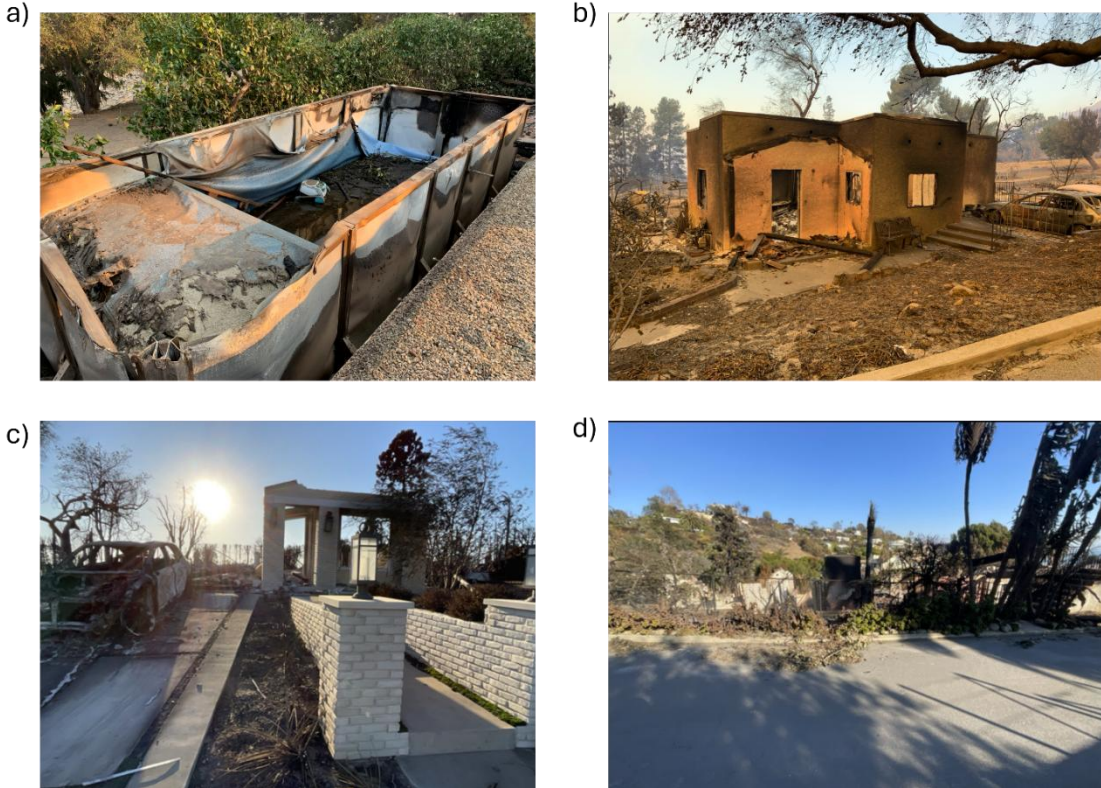


Figure 8: Pipeline Bs misclassification examples for destroyed for both front-view and multi-view: 5 (a) (Palisades), Figure 5 (b) (Palisades), Figure 5(c) (Eaton) and Figure 5(d) (Eaton). All homes in this figure had only a single view.



Figure 9. Cases in which both single view and multi-view were classified correctly in Pipeline b. Figure 6 (a–d) were classified as destroyed in ground truth labeling. All homes in this figure only had one single view. Figure 6(a) and (b) are in Eaton; Figure 6 (c) and (d) are in Palisades.

Figure 10 shows cases where the single view only images (a), (c), (e), and (g) (were classified as no damage; however, when the multi-view assessment was conducted, the household was classified as affected. Figure 10 (b), (d), (f), and (h) are the alternative views of houses (a), (c), (e), and (g), respectively. This shows the importance of having a workflow that is capable of processing multiple images.



Figure 10. In each row are pairs of images for the same house; front views of houses ((a), (c), (e), (g)) were classified as no damage. In the multi-view assessment, (a)–(b); (c)–(d); (e)–(f); and (g), (h) were inputs for the Pipeline B. They were classified as affected which matches the ground truth label.



Figure 11: The household in 11 (a – b) and 11 (d – f) were classified as no damage, but the ground truth was affected due to the broken glass. The household in 11 (c) was classified as affected due to the tarp being interpreted by debris; however, the ground truth was no damage.

Figure 11 shows cases where the household was misclassified for both pipelines; (a) and (b) are from the same household. Both models predicted no damage; however, broken glass is evident in Figure 8 (b) that caused ground truth to be classified as affected. The same case can be seen in Figure 8 (d), (e), and (f). These images from the same house, which were labeled as no damage for both views. The single view actually does not show any damage; however, broken glass is visible in Figure 8 (e) and (f), which was difficult for the model to identify, despite the prompt regarding the presence of broken glass. Future research can perhaps alter the brightness of the image to make the broken glass more identifiable. Figure 8 (c) had a ground truth label of no damage, but the object in front of the house led both views to predict damage since the prompt of regarding debris in front of the house was true. This demonstrates a tradeoff, as some images could have objects, such as tarp in this case, in front of the house and the model may classify the household as affected.

This visual analysis complements the findings in section 3.2 and section 3.3, specifically figure 10 shows the value of a multi-view image assessment. There are some cases where the model was not able to properly identify damage, specifically with broken glass as seen in figure 11. This limitation can be addressed in future studies with prompt engineering. Overall, the visual analysis was able to highlight how language models can improve damage classification.

4. Discussion

Ground level wildfire damage assessment is predominantly a manual task [15], despite tools that can improve the efficiency and accuracy of this process. This study proposes two pipelines that take advantage of the flexibility that language models can provide in wildfire damage assessment. The first pipeline is solely a VLM asked to classify post-fire images into three categories: no damage, affected, and destroyed. The second pipeline uses a VLM to assess if the damage indicators (highlighted in the appendix) are true/false based on the embedded image(s). This output is fed into an LLM that classifies a household's damage based on the damage indicators and embedded image. The findings showed that the affected category had poor F1 scores for both pipelines in Eaton and Palisades (Eaton Pipeline A: 0.429; Eaton

Pipeline B: 0.511; Palisades Pipeline A: 0.225; Palisades Pipeline B: 0.359) when assessing the front view only of the household. These scores improved significantly when multi-view images were assessed for both pipelines (Eaton Pipeline A: 0.920; Eaton Pipeline B: 0.947; Palisades Pipeline A: 0.857; Palisades Pipeline B: 0.891). Pipeline B showed potential for language prompting to enhance damage assessment; in all tests within this study, this pipeline outperformed Pipeline A. This is a promising sign as it can easily be used by practitioners for rapid damage assessment. They can save time and resources by having no need to train a model for wildfire rapid damage assessment.

The transition from pure vision-based models, such as vision transformers or convolutional neural networks, to vision-language models addresses critical limitations inherent in traditional approaches to multi-view damage assessment. Pure vision models typically demand extensive, labeled datasets for supervised training—a significant logistical barrier when rapid assessment is needed post-disaster. Furthermore, adapting these architectures to synthesize information from multiple perspectives is often computationally cumbersome, relying on methods like averaging image embeddings which can dilute localized damage signals. In contrast, the VLM workflow presented here utilizes pre-trained models (GPT-4o) with robust zero-shot capabilities, enabling immediate deployment without prior training. Crucially, VLMs are architecturally designed to process and reason over multiple visual inputs simultaneously. This allows the model to holistically assess a structure and identify damage not visible from the front (as demonstrated in Figure 7), directly leading to the substantial improvements observed in the affected category classification.

Beyond computational efficiency and accuracy, the integration of a large language model capabilities provides essential advantages in reasoning and adaptability that pure vision models lack. Traditional vision approaches often operate as "black boxes," learning complex features without explicit contextual grounding or interpretable justification. The VLM+LLM pipeline (Pipeline B), however, introduces a structured reasoning step where the model evaluates specific, domain-relevant damage indicators. This intermediate output provides a transparent, auditable rationale for the final classification based on the presence or absence of these indicators. Moreover, this prompt-based methodology offers unparalleled flexibility. Practitioners can rapidly fine-tune the assessment criteria by modifying the LLM prompts to reflect different hazard types, regional building practices, or evolving assessment standards, a process far more agile than retraining a specialized pure-vision architecture.

The proposed VLM and VLM+LLM pipelines are designed to enhance the efficiency of post-wildfire response, primarily serving as a tool for rapid triage and prioritization. The automated classifications generated by this workflow enable emergency managers to quickly gain situational awareness and identify areas with the most severe damage, facilitating faster allocation of resources and specialized assessment teams. It is crucial to emphasize that this automated assessment is not intended to replace the comprehensive evaluations conducted by certified inspectors for final damage determinations, insurance claims, or federal aid distribution. Instead, it aims to augment the preliminary damage assessment process by providing a scalable first-pass analysis.

5. Concluding Remarks

The second pipeline uses a VLM with LLM prompts to assess if damage indicators are true or false. Those outputs are fed into another VLM that classifies the image given the prompts. The findings show that the affected category had poor F1 scores for both pipelines in the Eaton Fire and Palisades Fire (Eaton Pipeline A: 0.429; Eaton Pipeline B: 0.511; Palisades Pipeline A: 0.225; Palisades Pipeline B: 0.359) when assessing the front view only of the household. These

scores improved significantly when multi-view images were assessed for both pipelines (Eaton Pipeline A: 0.920; Eaton Pipeline B: 0.947; Palisades Pipeline A: 0.857; Palisades Pipeline B: 0.891). Pipeline B showed potential for language prompting to enhance damage assessment. As in all tests in this study, Pipeline B outperformed Pipeline A. This result is a promising sign, as prompting could provide flexibility depending on the needs of practitioners. While the improvements were marginal, they could be enhanced in future studies. Therefore, the main practical contribution of this research is demonstrating how language models can process multiple views of a single household. This achievement was possible due to the fact that the study selected a pre-trained VLM, GPT-4o. Modern approaches, such as vision transformers, are data hungry and require huge amounts of labeled data for supervised training before it could be used for making classifications. By using VLM and LLM, we can finetune the workflow to adapt to the new settings on a very small sample dataset. The pipeline could be then used for making classifications.

The primary contribution of this work is a training-free, multi-view workflow that transforms ground-level images into auditable, indicator-guided damage assessments at the household level without requiring labeled datasets or custom multi-image fusion networks. The framework introduces three specific innovations. First, we operationalize household-level multi-view assessment within a pre-trained vision-language model, enabling comprehensive damage evaluation from multiple perspectives. Second, we implement a structured reasoning layer that extracts binary damage indicators prior to final classification, thereby enhancing both transparency and the ability to modify domain knowledge without retraining. Third, we provide explicit and reproducible design specifications, including the overall framework architecture, cosine-similarity methodology for consolidating minor, affected, and major damage categories, and detailed token-level computational and cost analysis. These components combine to create a deployable pipeline that practitioners can customize through simple prompt and indicator modifications rather than model retraining, significantly reducing barriers to rapid post-fire deployment while maintaining scientific rigor.

This framework provides preliminary damage assessment teams with an automated, immediately deployable capability that directly addresses two critical operational challenges identified in the introduction: the resource-intensive and slow nature of manual damage assessments and the limitations of aerial imagery in capturing parcel-level detail due to occlusion and resolution constraints. The systems multi-view approach recovers damage patterns invisible from façade perspectives alone, dramatically improving affected-class classification accuracy from approximately 1–36% with single views to 77–95% with multiple views across both fire events. This improvement enables rapid identification of properties requiring immediate inspection while reducing costly misclassifications of damaged structures as undamaged.

The systems reliance on pre-trained vision-language models, with an optional indicator stage, eliminates the need for local training data, allowing immediate deployment following a wildfire event. The paper provides comprehensive token-level cost analysis, revealing that Pipeline B requires approximately 150,000 additional tokens per 500-parcel assessment compared to Pipeline A, enabling agencies to make informed decisions balancing speed, interpretability, and budget constraints. Through multi-view ground-level imagery automation, this approach transforms dispersed photographic evidence into actionable, auditable assessments that complement aerial surveys and accelerate equitable resource allocation during the critical initial response phase following wildfire events.

Given the complexities inherent in structural damage assessment, a human-in-the-loop (HITL) approach remains essential for validation and accountability. While the multi-view assessment

significantly improved accuracy, the model may still struggle with subtle or ambiguous indicators. As observed in the visual analysis, indicators such as broken glass or the distinction of localized debris can sometimes lead to misclassifications. Therefore, outputs from the model, especially those classified as affected or cases where the model confidence is low, must be flagged for manual review by trained personnel. This hybrid approach ensures that the efficiencies of automation are realized without sacrificing the accuracy and nuanced understanding provided by human expertise.

Despite the promising results, this study has some limitations. A primary constraint is the reduced granularity of the damage assessment, necessitated by the aggregation of minor, major, and affected categories due to sample size limitations and high visual similarity between classes. This consolidation obscures nuanced differences critical for precise recovery planning. Furthermore, the visual analysis revealed challenges in the VLMs ability to interpret complex scenarios, such as misclassifying severely damaged but still-standing structures or failing to detect subtle indicators like broken glass. Finally, the current workflow relies exclusively on visual inputs, omitting contextual data that influences structural vulnerability, such as building materials, vegetation proximity, or localized fire intensity.

Future research should address these limitations by advancing the framework towards a truly multimodal system, integrating ground-level imagery with supplementary data sources like aerial imagery, geospatial data, and tabular structural characteristics. To improve the detection of nuanced damage and enhance classification granularity, advanced techniques such as retrieval-augmented generation should be explored. By grounding the LLMs reasoning in a knowledge base of forensic engineering guidelines and utilizing larger, more diverse datasets, the models capacity for fine-grained, context-aware damage classification can be significantly enhanced. Additionally, targeted fine-tuning of the VLM on specialized disaster imagery could improve sensitivity to subtle damage indicators.

Finally, the reliance on ground-level imagery necessitates strict adherence to data privacy protocols. While the images used in this study were sourced from a post-disaster damage inspection database, the broader deployment of GLI collection methods (e.g., crowdsourcing or rapid street-level captures) must adhere to ethical guidelines. Protocols must be established to anonymize any personally identifiable information captured incidentally in the imagery, such as faces, license plates, or house numbers, through blurring or redaction before images are processed and stored. This is vital to protect the privacy of residents during a vulnerable time.

Appendix

Table A1 presents the prompts that Pipeline B used. These prompts were inspired by literature that focused on building damage indicators after a wildfire occurs. Meldrum et al. (2022) provides a parcel level risk framework that describes how wildfire risk varies from home to home based on structural and fire characteristics (Meldrum et al., 2022). Chulahwat et al. (2023) how graph theory can be used for wildfire damage assessment and provides insight on what indicators to examine when assessing damage at the household level. The rationale behind these parameters are to guide the language model's decision-making process by adding domain knowledge. For example, vegetation is a key indicator of a household vulnerability to a fire (Chulahwat et al., 2022; Meldrum et al., 2022) ; therefore prompts relatives to vegetation should be included in this analysis. While the results in section 3.4 showed no statistical significance, it

provided future research to explore what methods can enhance classification while adding values le domain knowledge. Moreover, the prompts can be updated depending on the problems practitioners want to solve and has potential to add value in damage assessment literature.

Indicators	Literature
<i>is the house destroyed</i>	(Chulahwat et al., 2022)
<i>is the structure damaged</i>	(Chulahwat et al., 2022)
<i>is there any (even minor) damage visible on or around the house</i>	(Chulahwat et al., 2022)
<i>is there discoloration of walls or roof or around the house due to fire</i>	(Meldrum et al., 2022)
<i>are there any signs of even small affect due to fire</i>	(Meldrum et al., 2022)
<i>is the glass or windows broken</i>	(Meldrum et al., 2022)
<i>is the furniture burnt</i>	(Meldrum et al., 2022)
<i>are there burn marks on the structure</i>	(Meldrum et al., 2022)
<i>is the vegetation around burnt</i>	(Chulahwat et al., 2022)
<i>is the roof of the house damaged</i>	(Meldrum et al., 2022)
<i>is there debris around the house</i>	(Meldrum et al., 2022)

References

Ahmed, M. R., Rahaman, K. R., & Hassan, Q. K. (2018). Remote sensing of wildland fire-induced risk assessment at the community level. *Sensors (Switzerland)*, 18(5). <https://doi.org/10.3390/s18051570>

Chas-Amil, M. L., García-Martínez, E., & Touza, J. (2012). Fire risk at the wildland-urban interface: A case study of a Galician county. *WIT Transactions on Ecology and the Environment*, 158, 177–188. <https://doi.org/10.2495/FIVA120151>

Chen, K., & McAneney, J. (2004). Quantifying bushfire penetration into urban areas in Australia. *Geophysical Research Letters*, 31(12), 1–4. <https://doi.org/10.1029/2004GL020244>

Chulahwat, A., Mahmoud, H., Monedero, S., Diez Vizcaíno, F. J., Ramirez, J., Buckley, D., & Forradellas, A. C. (2022). Integrated graph measures reveal survival likelihood for buildings in wildfire events. *Scientific Reports*, 12(1), 1–12. <https://doi.org/10.1038/s41598-022-19875-1>

Dennison, Brewer, Arnold, M. (2014). Geophysical Research Letters. *Geophysical Prospecting, April*, 6298–6305. <https://doi.org/10.1002/2014GL059576>. Received

Diaz, N. D., Highfield, W. E., Brody, S. D., & Fortenberry, B. R. (2022). Deriving First Floor Elevations within Residential Communities Located in Galveston Using UAS Based Data. *Drones*, 6(4). <https://doi.org/10.3390/drones6040081>

Eaton, T. (2025). *Resilient Rebuilding : A Path Forward for Los Angeles*. 1–9.

Erni, S., Wang, X., Swystun, T., Taylor, S. W., Parisien, M. A., Robinne, F. N., Eddy, B., Oliver, J., Armitage, B., & Flannigan, M. D. (2024). Mapping wildfire hazard, vulnerability, and risk to Canadian communities. *International Journal of Disaster Risk Reduction*, 101(December 2023), 104221. <https://doi.org/10.1016/j.ijdrr.2023.104221>

Esparza, M., Ho, Y. H., Brody, S., & Mostafavi, A. (2025). Improving flood damage estimation by integrating property elevation data. *International Journal of Disaster Risk Reduction*, 118(July 2024), 105251. <https://doi.org/10.1016/j.ijdrr.2025.105251>

Galanis, M., Rao, K., Yao, X., Tsai, Y. L., Ventura, J., & Fricker, G. A. (2021). DamageMap: A post-wildfire damaged buildings classifier. *International Journal of Disaster Risk Reduction*, 65, 102540. <https://doi.org/10.1016/j.ijdrr.2021.102540>

Gao, G., Ye, X., Li, S., Huang, X., Ning, H., Retchless, D., & Li, Z. (2024). Exploring flood mitigation governance by estimating first-floor elevation via deep learning and google street view in coastal Texas. *Environment and Planning B: Urban Analytics and City Science*, 51(2), 296–313. <https://doi.org/10.1177/23998083231175681>

Ho, Y.-H., Lee, C.-C., Diaz, N., Brody, S., & Mostafavi, A. (2024). ELEV-VISION: Automated Lowest Floor Elevation Estimation from Segmenting Street View Images. *ACM Journal on Computing and Sustainable Societies*, 2(2). <https://doi.org/10.1145/3661832>

Ho, Y.-H., Li, L., & Mostafavi, A. (2024). *ELEV-VISION-SAM: Integrated Vision Language and Foundation Model for Automated Estimation of Building Lowest Floor Elevation*. 2010. <http://arxiv.org/abs/2404.12606>

Insurance Institute for Business and Home Safety. (2024). *The 2023 Lahaina Conflagration. September*.

Iván Higuera-Mendieta, Jeff Wen, M. B. (2023). *A table is worth a thousand pictures : Multi-modal contrastive learning in house burning classification in wildfire events*.

Lee, J., Xu, J. Z., Sohn, K., Lu, W., Berthelot, D., Gur, I., Khaitan, P., Ke-Wei, Huang, Koupparis, K., & Kowatsch, B. (2020). *Assessing Post-Disaster Damage from Satellite Imagery using Semi-Supervised Learning Techniques*. 1–10. <http://arxiv.org/abs/2011.14004>

Luo, K., & Lian, I. Bin. (2024). Building a Vision Transformer-Based Damage Severity Classifier with Ground-Level Imagery of Homes Affected by California Wildfires. *Fire*, 7(4). <https://doi.org/10.3390/fire7040133>

Mahmoud, H. (2024). Reimagining a pathway to reduce built-environment loss during wildfires. *Cell Reports Sustainability*, 1(6), 100121. <https://doi.org/10.1016/j.crsus.2024.100121>

Mahmoud, H., & Chulahwat, A. (2018). Unraveling the Complexity of Wildland Urban Interface Fires. *Scientific Reports*, 8(1), 1–12. <https://doi.org/10.1038/s41598-018-27215-5>

Mall, U., Phoo, C. P., Liu, M. K., Vondrick, C., Hariharan, B., & Bala, K. (2024). Remote Sensing Vision-Language Foundation Models Without Annotations Via Ground Remote Alignment. *12th International Conference on Learning Representations, ICLR 2024*, 1–22.

Meldrum, J. R., Barth, C. M., Goolsby, J. B., Olson, S. K., Gosey, A. C., White, J., Brenkert-Smith, H., Champ, P. A., & Gomez, J. (2022). Parcel-Level Risk Affects Wildfire Outcomes: Insights from Pre-Fire Rapid Assessment Data for Homes Destroyed in 2020 East Troublesome Fire. *Fire*, 5(1). <https://doi.org/10.3390/fire5010024>

Nia, K. R., & Mori, G. (2017). Building damage assessment using deep learning and ground-level image data. *Proceedings - 2017 14th Conference on Computer and Robot Vision, CRV 2017, 2018-Janua*, 95–102. <https://doi.org/10.1109/CRV.2017.54>

Salvati, L. (2014). Profiling forest fires along the urban gradient: a Mediterranean case study. *Urban Ecosystems*, 17(4), 1175–1189. <https://doi.org/10.1007/s11252-014-0359-y>

Sarricolea, P., Serrano-Notivoli, R., Fuentealba, M., Hernández-Mora, M., de la Barrera, F., Smith, P., & Meseguer-Ruiz, Ó. (2020). Recent wildfires in Central Chile: Detecting links between burned areas and population exposure in the wildland urban interface. *Science of the Total Environment*, 706, 135894. <https://doi.org/10.1016/j.scitotenv.2019.135894>

Taccaliti, F., Marzano, R., Bell, T. L., & Lingua, E. (2023). *Wildland – Urban Interface : Definition and Physical Fire Risk Mitigation Measures , a Systematic Review*.

Wang, J., Xuan, W., Qi, H., Liu, Z., Liu, K., & Wu, Y. (n.d.). *DisasterM3 : A Remote Sensing Vision-Language Dataset for Disaster Damage Assessment and Response*. 1–12.

Wang, W., Zhao, F., Wang, Y., Huang, X., & Ye, J. (2023). Seasonal differences in the spatial patterns of wildfire drivers and susceptibility in the southwest mountains of China. *Science of the Total Environment*, 869(August 2022), 161782. <https://doi.org/10.1016/j.scitotenv.2023.161782>

Wheeler, B. J., & Karimi, H. A. (2020). Deep learning-enabled semantic inference of individual building damage magnitude from satellite images. *Algorithms*, 13(8). <https://doi.org/10.3390/A13080195>

Xie, B., Xu, J., Jung, J., Yun, S. H., Zeng, E., Brooks, E. M., Dolk, M., & Narasimhalu, L. (2020). Machine Learning on Satellite Radar Images to Estimate Damages after Natural Disasters.

GIS: Proceedings of the ACM International Symposium on Advances in Geographic Information Systems, 461–464. <https://doi.org/10.1145/3397536.3422349>

Yang, Y., Zou, L., Zhou, B., Li, D., Lin, B., Abedin, J., & Yang, M. (2025). Hyperlocal disaster damage assessment using bi-temporal street-view imagery and pre-trained vision models. *Computers, Environment and Urban Systems*, 121(August), 102335. <https://doi.org/10.1016/j.compenvurbsys.2025.102335>

Zhai, W., & Peng, Z. R. (2020). Damage assessment using Google Street View: Evidence from Hurricane Michael in Mexico Beach, Florida. *Applied Geography*, 123(July), 102252. <https://doi.org/10.1016/j.apgeog.2020.102252>